DOI: 10.61782/fa.2023.0866

forum acusticum 2023

MODIFIABLE LABYRINTHINE MICROSTRUCTURE FOR ADJUSTABLE SOUND ABSORPTION AND INSULATION

Kamil C. Opiela* **Tomasz G. Zieliński**
Department of Intelligent Technologies, Institute of Fundamental Technological Research, Polish Academy of Sciences, Poland

ABSTRACT

Materials with open porosity are known to absorb sound very well. However, their efficiency in acoustic absorption and insulation is sometimes restricted to specific frequency ranges. It is possible to circumvent this drawback by designing a porous microstructure that can be modified on the fly and thereby enabling the change in its crucial geometrical parameters like tortuosity that influence the intensity of viscous energy dissipation phenomena taking place on a microscale. A prototype of such a material consisting of relocatable small steel balls embedded in a periodic rigid skeleton is devised and additively manufactured in separate pieces in the stereolithography technology. The balls are inserted into proper places manually. The full sample is then assembled and its acoustic characteristics are determined computationally and experimentally using dual-scale, unit-cell analyses and impedance-tube measurements, respectively. The resulting material is shown to possess two extreme spectra of normal incidence sound absorption coefficient and transmission loss that are dependent on the particular position of balls inside the microstructure. In consequence, acoustic waves from a much larger frequency range can be effectively absorbed or insulated by a relatively thin material layer compared to a similar design without movable balls.

Keywords: *sound absorption, sound transmission, modifiable porous microstructure, additive manufacturing*

**Corresponding author*: *kopiela@ippt.pan.pl.*

1. INTRODUCTION

The concept of an adaptable sound absorber with modifiable microstructure was introduced in [1] and then demonstrated in [2, 3]. The general principle of its operation lies in the fact that the acoustic properties of rigid porous materials depend solely on their microgeometry and macroscopic thickness, given certain sound incidence conditions and fluid filling the pores. In the aforementioned papers, the thickness and the direction of acoustic wave propagation were fixed. The normal incidence sound absorption spectra of the proposed materials were changeable in the wake of the relocation of steel balls present in their microstructures that influence their crucial geometric features.

This contribution includes the results of modelling and experimental investigation of normal incidence sound absorption coefficient and transmission loss obtained for a dual-purpose porous material. Thanks to its design and in particular movable steel balls inserted into its main pores, the material possesses two extreme states: the first oriented on sound absorption, and the second focused on effective sound insulation. The tests conducted on an additively manufactured prototype showed good correspondence between predictions and measurements. In contrast to conventional acoustic foams, the adaptable material reveals very good sound absorption and transmission loss characteristics simultaneously.

2. MODIFIABLE POROUS MICROSTRUCTURE

Figure 1a presents the periodic representative fragment of the skeleton from which the porous adaptable material is constructed. The representative skeleton fragment is composed of two 3 mm × 3 mm × 3 mm parts with:

1. a centrally located main spherical pore of diameter

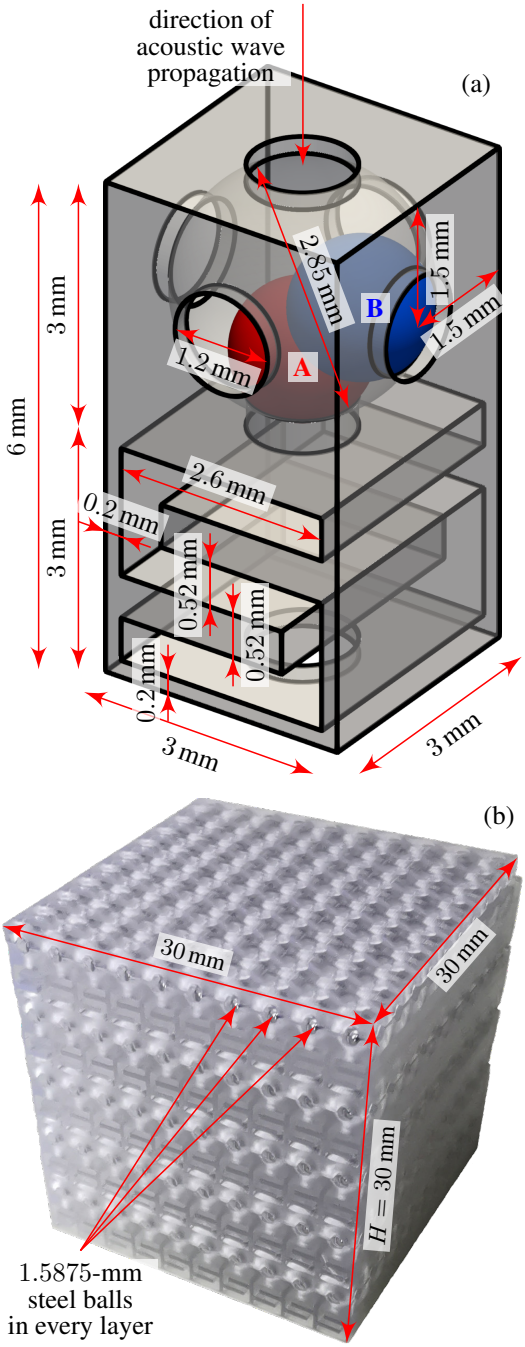

Figure 1: Porous microgeometry: (a) the representative periodic skeleton fragment with two considered ball positions; (b) the photograph of the additively manufactured sample containing small steel balls.

2.85 mm as well as six 1.2-mm vertical and horizontal cylindrical channels that guarantee openness of the whole porous network. Importantly, in the main pore there is a single perfectly spherical steel ball of diameter 1.5875 mm in one of two positions: A (blocking the propagation of acoustic waves in the vertical channel oriented along the direction of sound incidence) or B (blocking the propagation in the horizontal channel);

2. a regular straight labyrinthine channel of width 0.52 mm—three horizontal slits of length 2.6 mm separated by solid strips of thickness 0.52 mm and joined together by 0.52 mm-wide links.

The real imperfect channel-closing conditions were imitated by leaving a 0.015-mm radial gap between the ball and solid skeleton.

A 30 mm × 30 mm × 30 mm cuboidal sample of the proposed material, shown in Figure 1b, was additively manufactured in the stereolithography technology (photocuring of liquid polymer resin). It was assembled from five individually printed rigid layers containing 10 × 10 representative skeleton fragments shifted by 1/4 of the period to facilitate manual steel ball insertion. One layer was fabricated in two parts which were placed at the bottom and top of the sample. The three-dimensional geometrical models involved were created in FreeCAD [4].

3. METHODS

The acoustic indicators of interest were predicted using the micro-macro equivalent-fluid approach for rigid-frame porous media [5]. The method relies on introducing a homogenised fluid with the equivalent density $\varrho_{\text{eq}}(f)$ and equivalent bulk modulus $K_{\text{eq}}(f)$ (f is the temporal frequency) in place of the open-porosity material. For air saturating the medium, these two complex-valued frequency-dependent properties can be expressed as:

$$\varrho_{\text{eq}}(f) = \frac{\varrho_{\text{air}}\alpha}{\phi} \tag{1}$$

and

$$K_{\text{eq}}(f) = \frac{K_{\text{air}}}{\phi}\left(\gamma_{\text{air}} - \frac{\gamma_{\text{air}} - 1}{\alpha'}\right)^{-1}, \tag{2}$$

where $\varrho_{\text{air}} = 1.204\,\text{kg/m}^3$ denotes the density of air, $K_{\text{air}} = 141855\,\text{Pa}$ is its bulk modulus, and $\gamma_{\text{air}} = 1.4$ is the ratio of specific heats for air. The dynamic visco-inertial tortuosity $\alpha(f)$ and dynamic thermal tortuosity $\alpha'(f)$ are estimated using the well-known

Table 1: The numerical JCALP parameters for the adaptable structure with two extreme ball positions.

Parameter	Symbol	Unit	Ball position	
			A	B
Open porosity	ϕ	–	0.467	0.467
Static viscous permeability	k_0	$10^{-9}\,\mathrm{m}^2$	0.024	3.121
Static thermal permeability	k_0'	$10^{-9}\,\mathrm{m}^2$	22.55	22.3
Kinematic tortuosity	α_∞	–	5.082	3.719
Static viscous tortuosity	α_0	–	6.402	4.971
Static thermal tortuosity	α_0'	–	1.849	1.818
Viscous characteristic length	Λ	mm	0.0998	0.44
Thermal characteristic length	Λ'	mm	0.584	0.584

Johnson-Champoux-Allard-Lafarge-Pride (JCALP) semi-phenomenological model [5], i.e. as functions of eight geometric parameters, namely the open porosity ϕ, static viscous permeability k_0, static thermal permeability k_0', kinematic tortuosity α_∞, static viscous tortuosity α_0, static thermal tortuosity α_0', viscous characteristic length Λ, and thermal characteristic length Λ':

$$\alpha(f) = \alpha(f;\, \phi, \alpha_\infty, \alpha_0, k_0, \Lambda)\,, \tag{3}$$

$$\alpha'(f) = \alpha'(f;\, \phi, \alpha_0', k_0', \Lambda')\,. \tag{4}$$

The JCALP model is sophisticated enough to account for pores with possible constrictions between them.

At normal incidence, the sound absorption coefficient for a material layer of thickness H is determined as:

$$\mathcal{A}(f) = 1 - \left| \frac{Z - Z_{\mathrm{air}}}{Z + Z_{\mathrm{air}}} \right|^2, \tag{5}$$

where

$$Z(f) = -\mathrm{i}\, Z_{\mathrm{eq}} \cot\left(2\pi f H \frac{1}{c_{\mathrm{eff}}}\right) \tag{6}$$

is the surface acoustic impedance, $Z_{\mathrm{air}} = \sqrt{\varrho_{\mathrm{air}} K_{\mathrm{air}}}$ is the characteristic impedance of air, i is the imaginary unit, $Z_{\mathrm{eq}}(f) = \sqrt{\varrho_{\mathrm{eq}} K_{\mathrm{eq}}}$ is the equivalent characteristic impedance, and $c_{\mathrm{eff}}(f) = \sqrt{K_{\mathrm{eq}}/\varrho_{\mathrm{eq}}}$ is the effective speed of sound in the homogenised medium.

The sound transmission loss at normal incidence is also determined from the equivalent-fluid properties. It is given by:

$$\mathcal{TL}(f) = -10 \log_{10} \mathcal{T}\,, \tag{7}$$

where

$$\mathcal{T}(f) = |\mathcal{TF}|^2 \tag{8}$$

is the so-called sound transmission coefficient and

$$\mathcal{TF}(f) = \frac{2}{2\cos(2\pi f H \frac{1}{c_{\mathrm{eff}}}) + \mathrm{i}\,(\frac{Z_{\mathrm{eq}}}{Z_{\mathrm{air}}} + \frac{Z_{\mathrm{air}}}{Z_{\mathrm{eq}}})\sin(2\pi f H \frac{1}{c_{\mathrm{eff}}})} \tag{9}$$

is the sound transmission factor.

The sound absorption coefficient and sound transmission loss at normal incidence were also obtained experimentally from acoustic pressure readings in a square 30-mm impedance tube in accordance with the standards described in [6, 7] and [8], respectively. During the measurements the impedance tube was mounted either horizontally or vertically to ensure proper position of the balls.

4. RESULTS

The values of the numerically calculated geometric parameters of the microstructure are given in Table 1. The relevant formulas for them are reported e.g. in [9] or [10]. The necessary three-dimensional, stationary, finite-element analyses with up to 1227288 degrees of freedom were run in the FEniCS v2019.1.0 [11] open-source computing platform on a half of the periodic domain occupied by air saturating the representative skeleton fragment (see Figure 1a), taking advantage of problem symmetry. Two tetrahedral meshes refined near solid skeleton walls with about 62000 vertices and 220000 elements were prepared for this purpose. As a consequence of the ball relocation within the main pore from position A to B, the static viscous permeability increases 130 times, the viscous characteristic length is more than 4 times larger, kinematic tortuosity and static viscous tortuosity drop significantly, whereas the other parameters do not change or are nearly the same.

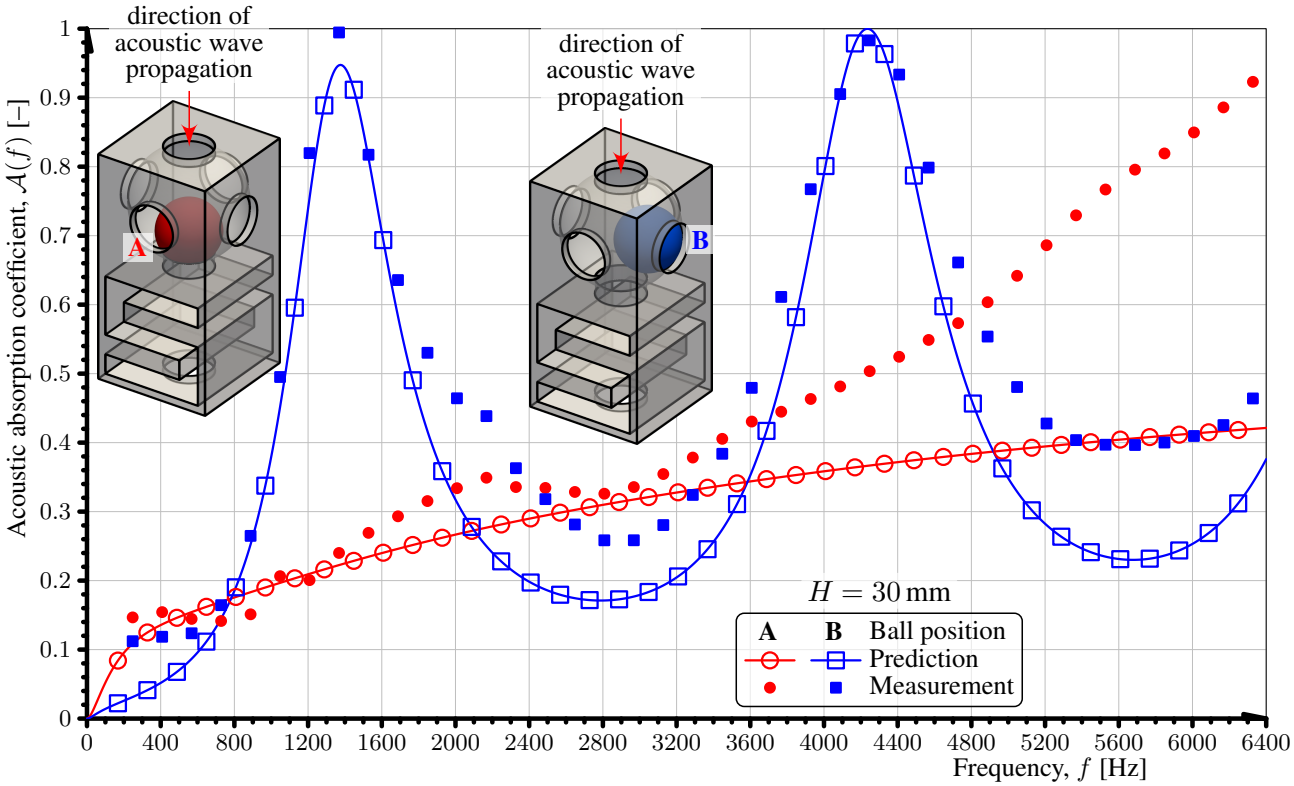

Figure 2: Measured and predicted normal incidence sound absorption coefficient spectra for a 30 mm-thick hard-backed layer of the adaptable material with two extreme ball positions.

Figures 2 and 3 present normal incidence sound absorption coefficient and transmission loss spectra, respectively, measured and predicted for the manufactured sample. The experimental results in the frequency range up to 6.4 kHz indicate that the material provides high sound insulation from about 20 dB to 65 dB when the balls are in position A (the vertical channels oriented along the direction of sound incidence are blocked), and is an efficient sound absorber with perfect absorption around 1250 Hz and 4.2 kHz when the balls are in position B (horizontal channels are blocked). Generally, the two considered acoustic indicators are accurately predicted with considerable sound absorption and insulation discrepancies above, say, 4 kHz mainly for the case of the ball closing the vertical channel (in position A).

5. CONCLUSIONS

The research conducted led to the following conclusions:

- It is possible to design and additively manufacture a sample of an adaptable porous material that for certain noise conditions is effective both in sound absorption and sound insulation.
- When the balls are in position A and block the vertical channels oriented along the direction of sound incidence, air tends to flow mainly parallelly to the layers from which the sample is assembled. Moreover, in reality the channel closing is not perfect and some portion of the airflow is directed through a small gap between the ball and solid skeleton. This in turn results in bigger discrepancies between the experimental data and idealised predictions.
- The nature of the sound absorption coefficient and transmission loss spectra is well-predicted when the balls are in position B, that is when they do *not* block the channels oriented along the direction of incidence. In this case the main harmonic airflow is perpendicular to the layers of the sample there-

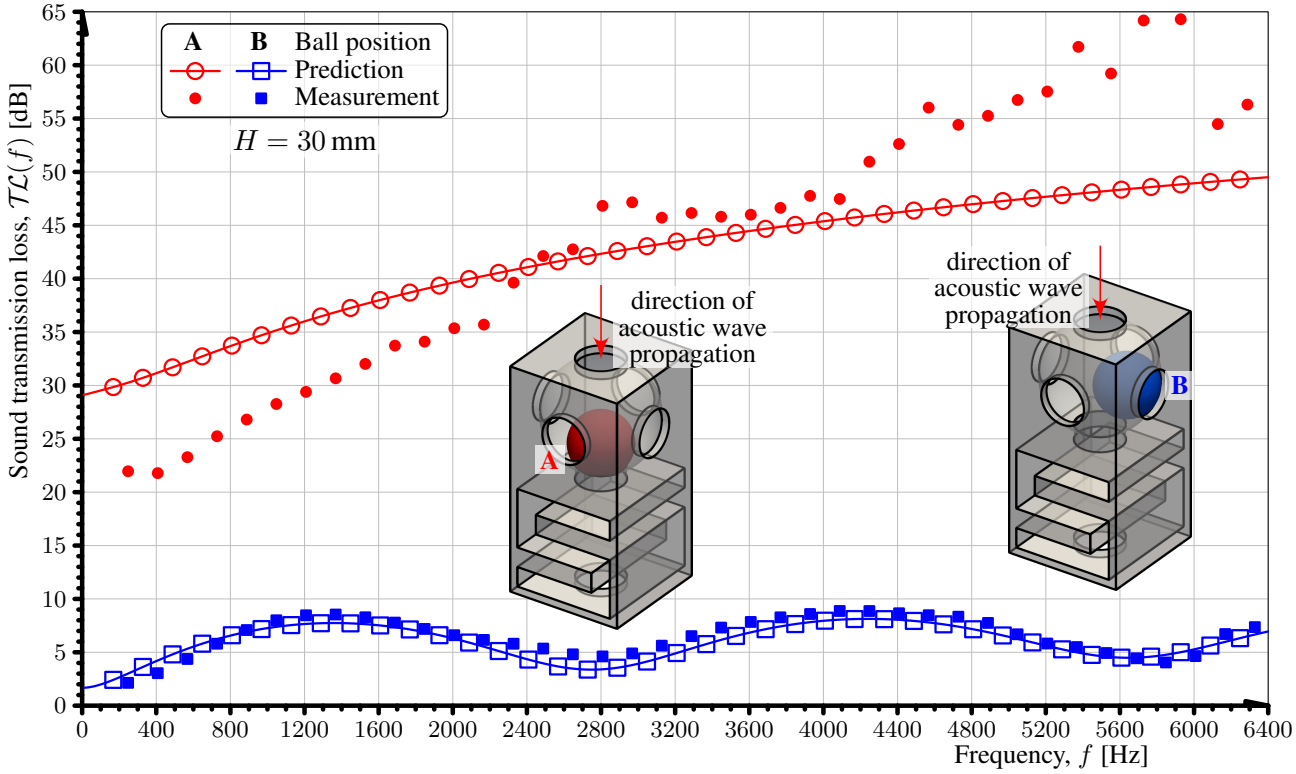

Figure 3: Measured and predicted normal incidence sound transmission loss spectra for a 30 mm-thick layer of the adaptable material with two extreme ball positions.

fore minimising sound leakages due to imperfect connections.

- The underestimated sound absorption between absorption peaks for the ball position B is attributed to various manufacturing flaws like dimensional inaccuracy or surface roughness that intensify viscous losses in general.

6. ACKNOWLEDGMENTS

The financial support of the project number 2020/37/N/ST8/04071: "Impact of the 3D printing process on the acoustic properties of porous materials", financed by the National Science Centre, Poland, is gratefully acknowledged.

7. REFERENCES

[1] K. C. Opiela, M. Rak, and T. G. Zieliński, "A concept demonstrator of adaptive sound absorber/insulator involving microstructure-based modelling and 3D printing," in *Proc. of ISMA2018 International Conference on Noise and Vibration Engineering/USD2018 International Conference on Uncertainty in Structural Dynamics* (W. Desmet, B. Pluymers, D. Moens, and W. Rottiers, eds.), (Heverlee, Belgium), pp. 1091–1104, Katholieke Universiteit Leuven, Department of Mechanical Engineering, Sept. 2018.

[2] K. C. Opiela and T. G. Zieliński, "Microstructural design, manufacturing and dual-scale modelling of an adaptable porous composite sound absorber," *Compos. Pt. B-Eng.*, vol. 187, pp. 1–13, article 107833, Apr. 2020.

[3] K. C. Opiela, R. Konowrocki, and T. G. Zieliński, "Magnetically controlled sound absorption by means of a composite additively manufactured material," in *7th European Conference on Structural Control: Book of Abstracts and Selected Papers* (J. Holnicki-Szulc, D. Wagg, Ł. Jankowski, B. Błachowski, and P. Tau-

zowski, eds.), (Warsaw, Poland), pp. 153–154, Institute of Fundamental Technological Research and Committee on Mechanics, Polish Academy of Sciences, July 2022.

[4] "FreeCAD (version 0.20.2)." `https://www.freecad.org/`. Accessed: 15 May 2023.

[5] J.-F. Allard and N. Atalla, *Propagation of sound in porous media: Modelling sound absorbing materials*. John Wiley & Sons, 2 ed., Oct. 2009.

[6] ASTM E1050-12, "Standard test method for impedance and absorption of acoustical materials using a tube, two microphones and a digital frequency analysis system," ASTM standard, ASTM International, 100 Barr Harbor Drive, PO Box C700, West Conshohocken, PA 19428-2959, United States.

[7] ISO 10534-2, "Acoustics — Determination of sound absorption coefficient and impedance in impedance tubes — Part 2: Transfer-function method," ISO standard, International Organisation for Standardization, Case postale 56, CH-1211 Genève 20, Switzerland, Nov. 1998.

[8] ASTM E2611-17, "Standard test method for normal incidence determination of porous material acoustical properties based on the transfer matrix method," ASTM standard, ASTM International, 100 Barr Harbor Drive, PO Box C700, West Conshohocken, PA 19428-2959, United States.

[9] K. C. Opiela, T. G. Zieliński, and K. Attenborough, "Limitations on validating slitted sound absorber designs through budget additive manufacturing," *Mater. Des.*, vol. 218, pp. 1–17, article 110703, June 2022.

[10] T. G. Zieliński, R. Venegas, C. Perrot, M. Červenka, F. Chevillotte, and K. Attenborough, "Benchmarks for microstructure-based modelling of sound absorbing rigid-frame porous media," *J. Sound Vibr.*, vol. 483, pp. 1–38, article 115441, Sept. 2020.

[11] M. S. Alnæs, J. Blechta, J. Hake, A. Johansson, B. Kehlet, A. Logg, C. Richardson, J. Ring, M. E. Rognes, and G. N. Wells, "The FEniCS Project version 1.5," *Arch. Num. Softw.*, vol. 3, pp. 9–23, Dec. 2015.